Regioselective Hydroformylation of Internal and Terminal Alkenes via Remote Supramolecular Control

Linnebank, P.R.; Ferreira, S.F.; Kluwer, A.M.; Reek, J.N.H.

DOI
10.1002/chem.202000620

Publication date
2020

Document Version
Final published version

Published in
Chemistry-A European Journal

Chemistry–A European Journal
Communication
doi.org/10.1002/chem.202000620

Chemistry Europe
European Chemical Societies Publishing

Supramolecular Chemistry |*Hot Paper*|

Regioselective Hydroformylation of Internal and Terminal Alkenes via Remote Supramolecular Control

Pim R. Linnebank,[a] Stephan Falcão Ferreira,[a] Alexander M. Kluwer,[b] and Joost N. H. Reek*[a, b]

Abstract: Regioselective catalytic transformations using supramolecular directing groups are increasingly popular as it allows for control over challenging reactions that may otherwise be impossible. In most examples the reactive group and the directing group are close to each other and/or the linker between the directing group is very rigid. Achieving control over the regioselectivity using a remote directing group with a flexible linker is significantly more challenging due to the large conformational freedom of such substrates. Herein, we report the redesign of a supramolecular Rh–bisphosphite hydroformylation catalyst containing a neutral carboxylate receptor (DIM pocket) with a larger distance between the phosphite metal binding moieties and the DIM pocket. For the first time regioselective conversion of internal and terminal alkenes containing a remote carboxylate directing group is demonstrated. For carboxylate substrates that possess an internal double bond at the Δ-9 position regioselectivity is observed. As such, the catalyst was used to hydroformylate natural monounsaturated fatty acids (MUFAs) in a regioselective fashion, forming of an excess of the 10-formyl product (10-formyl/9-formyl product ratio of 2.51), which is the first report of a regioselective hydroformylation reaction of such substrates.

Supramolecular approaches in transition metal catalysis offer unique tools to achieve selectivity in transformations that are otherwise difficult to control.[1–8] Unrivalled selectivity by supramolecular strategies has been demonstrated for a wide array of organic and organometallic transformations.[9–28] A frequently applied strategy involves the use of a functional group on a substrate that serves as a directing group to control the substrate coordination at the metal center, allowing for differentiation of reactive sites that are otherwise indistinguishable for transition metal catalysts. This strategy, coined substrate preorganization, has been broadly demonstrated for substrates in which the directing group is relatively close to the reactive group.[13,14,22–26] It remains an open question if such a strategy can be extended to substrates in which the functional group is remote from the directing group, which may be especially challenging for long flexible alkyl chain type substrates due to the large conformational freedom of such compounds.

Recently, Costas et al. reported a system in which protonated aliphatic amines were oxidized by a manganese catalyst functionalized with crown ether recognition sites, leading to selective oxidation of the C–H carbons to yield a mixture of position 8 and 9 oxidation products using substrate preorganization.[28]

Toste et al. reported a transition metal catalyst encapsulated in a self-assembled cage that can be used for site selective hydrogenation of polyenes.[16] Moreover, the selectivity in hydroformylation reactions can also be controlled by substrate preorganization via carboxylate directing groups. The guanidinium functionalized monodentate phosphine ligands introduced by Breit et al. convert terminal and internal alkenes to the outermost aldehyde with high regioselectivity, provided that the carboxylic acid and alkene are in close distance.[24] Our group reported the regioselective hydroformylation of unsaturated carboxylates using bisphosphine and bisphosphite ligands, which contained a neutral anion receptor based on 7,7′-diamido-2,2′-diindolylmethane (DIM pocket).[20–23,29] This class of ligands was coined DIMPhos. The rhodium–DIMPhos catalyst based on **L1** (Figure 1a) hydroformylates internal alkenes such as 4-hexenoate with high regioselectivity (78:1 selectivity) but for longer substrates the regioselectivity is much lower and application of **L1** in the hydroformylation of natural fatty acids with a double bond on the 9-position gives no regioselectivity (vide infra).[22] Currently there are no hydroformylation catalysts that convert natural monounsaturated fatty acids (MUFAs) in a regioselective fashion, whereas such technologies may allow broader applicability of the biofeedstock.[30–42]

In this paper we report the redesign of DIMPhos ligand **L1** to **L2** in which the distance between the active metal and the binding site matches that of typical natural fatty acids (Figure 1a), and demonstrate that the concept of substrate orientation to control the regioselectivity in hydroformylation also works when the directing group is remote from the double bond.

The distance between rhodium and the 7,7′-diamido-2,2′-diindolylmethane anion receptor for **L1** (the DIM pocket, 6.8 Å,

[a] P. R. Linnebank, S. F. Ferreira, Prof. Dr. J. N. H. Reek
Homogeneous, Supramolecular and Bio-Inspired Catalysis
Van't Hoff Institute for Molecular Sciences University of Amsterdam
Science Park 904, 1098 XH Amsterdam (The Netherlands)
E-mail: j.n.h.reek@uva.nl

[b] A. M. Kluwer, Prof. Dr. J. N. H. Reek
InCatT B.V.
Science Park 904, 1098 XH Amsterdam (The Netherlands)

Supporting information and the ORCID identification number(s) for the author(s) of this article can be found under:
https://doi.org/10.1002/chem.202000620.

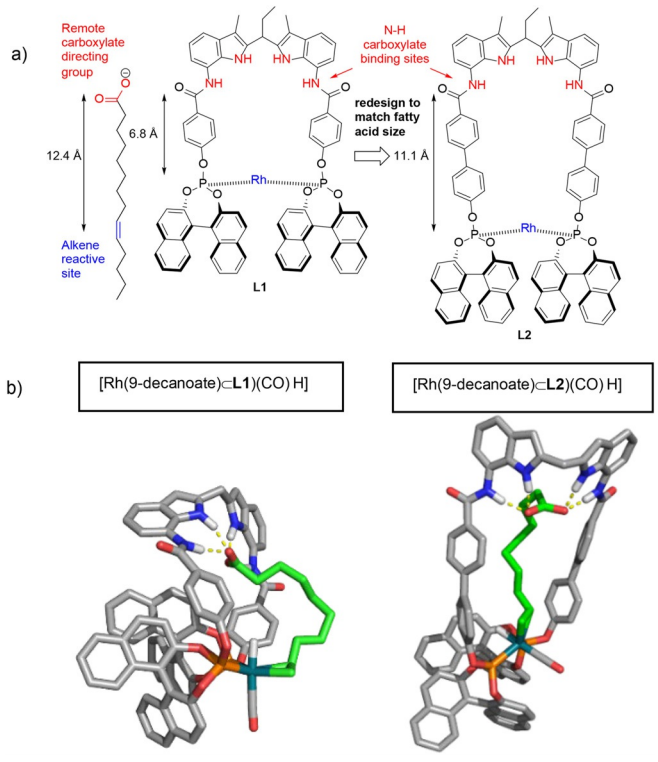

Figure 1. a) Redesign of a rhodium-monophenyl (**L1**) to a rhodium biphenyl (**L2**) DIMPhos complex to match the distance between the acid directing group and alkene functionality in typical fatty acids. b) Modeling (DFT) of 9-decanoate as a fatty acid model bound ditopically to [Rh(**L1**)(H)(CO)] (left) and [Rh(**L2**)(H)(CO)] (right). For clarity, the 9-decanoate substrate is shown in green.

Figure 1 a) is significantly shorter than the carboxylate-alkene distance of fatty acids (12.4 Å) and this mismatch was proposed to be the reason for the low selectivity observed for long substrates (vide infra).[22] Indeed, DFT calculations (BLYP,DZP,D3BJ) show that 9-decenoate, used as a model for natural fatty acids, needs to fold significantly to bind ditopically to [Rh(**L1**)(H)(CO)] (see Figure 1 b).[43–45] It was hypothesized that an extended ligand binds substrates with large carboxylate-alkene distances in less folded manners and as a result leads to a higher control over the regioselectivity. To achieve this goal, we designed a ligand that has a biphenyl linker (Figure 1 a, **L2**) between the DIM pocket and the phosphite donor atoms, instead of the phenyl linker that is present in the original DIMphos ligand (**L1**). DFT calculations of 9-decenoate ditopically bound to [Rh(**L2**)(H)(CO)] (Figure 1 b) indeed shows less folding compared to binding to [Rh(**L1**)(H)(CO)]. This is also reflected in the lower folding energy of 9-decenoate bound to a [Rh(**L2**)(H)(CO)] (9.4 kcal mol^{-1} for [Rh(9-decenoate)⊂**L2**)(CO)H] vs. 15.4 kcal mol^{-1} for [Rh(9-decenoate)⊂**L1**)(CO)H] (see Table S6 in the Supporting Information). Also binding enthalpies of aliphatic deprotonated ω-unsaturated carboxylic acids with various lengths (3-butenoate to 10-undecenoate) to [Rh(**L2**)(H)(CO)] were calculated using DFT (see Figure S74). These studies show that 8-nonenoate fits best and has the highest binding enthalpy. In addition, 9-decenoate, which is a better model for natural fatty acids, also binds well to [Rh(**L2**)(H)(CO)]. Encouraged by these results, we synthesized the **L2** ligand using a similar synthetic strategy as previously reported for **L1** (see Supporting Information).[22]

To investigate if ligand **L2** formed a stable metal complex with rhodium it was mixed with [Rh(acac)(CO)$_2$], which is the precursor complex of the hydroformylation catalyst, in a 1:1 ratio in CD_2Cl_2. ^{1}H NMR studies show a well-defined complex formed after mixing (see Figure S2) and DOSY spectroscopy reveals the formation of a single species with a hydrodynamic radius of 7.9 Å in line with the size of a mononuclear complex (see Figure S3).[46] Upon addition of 1.5 equivalents of tetrabutylammonium acetate, the N-H protons are downfield shifted, which shows the carboxylate group binds to the DIM pocket of the [Rh(acac)(**L2**)] in a similar fashion as reported for complex [Rh(acac)(**L1**)] (Figure S4).[21] Pressurization with 5 bar of syngas (H_2:CO (1:1)) to the solution of the [Rh(acac)(**L2**)] complex provides the corresponding pentacoordinate [Rh(**L2**)-(CO)$_2$H] species as evidenced by the rhodium hydrido signal ($\delta = -10.5$ ppm).[47] Next to the well-defined signal, also a broad rhodium–hydrido signal ($\delta = -10.7$ ppm) appears in the NMR spectrum, which becomes larger over time (see Figure S4). DOSY spectroscopy of the [Rh(**L2**)(CO)$_2$H] complex under 5 bar CO/H_2 (1:1) in CD_2Cl_2 gave a larger average hydrodynamic radius (12.1 Å) than for the [Rh(acac)(**L2**)] complex suggesting that the broad signal is due to formation of dinuclear and/or oligomeric species under these conditions (see Figure S10). However, under identical conditions but in the presence of 4 equivalents guest that binds in the DIMpocket (tetrabutylammonium acetate) the average hydrodynamic radius (8.4 Å) (see Figure S11) is close to that of the [Rh(acac)-(**L2**)] species, indicating that carboxylate binding in the DIM pocket preorganizes the two phosphorous moieties for the formation of mononuclear species.[29]

A series of (deprotonated) ω-unsaturated carboxylic acids with varying length between the alkene reactive group and the carboxylate directing group was hydroformylated using [Rh(**L2**)] as a catalyst (Figure 2). As substrates we reacted 4-pentenoic acid ($n = 2$) up to 10-undecenoic acid ($n = 8$) both in the presence and the absence of base.

In the presence of base, the carboxylate functional group of the substrate binds in the DIM pocket and thus substrates long enough to span the DIM pocket-rhodium distance are expected to react with improved regioselectivity. In absence of base, the protonated carboxylic acids do not bind in the DIM pocket and as a result the directing group, the carboxylic acid, cannot be used for substrate preorganization with the [Rh(**L2**)] catalyst and should react with lower regioselectivity.[20,21] Because of this, the protonated substrates were used as control experiments. All substrates studied gave full conversion to the aldehyde and the linear/branched (l/b) ratios of the aldehyde products were determined by ^{1}H-NMR spectroscopy (Figure 2). The catalytic results show that the long anionic substrates (with $n > 4$, 7-octenoate and longer) display much higher l/b ratios than the protonated analogues. The distance between the carboxylate and alkene function in these substrates is at least 9.7 Å, and this shows this catalyst is able to control the regioselectivity via substrate preorganization on remote dis-

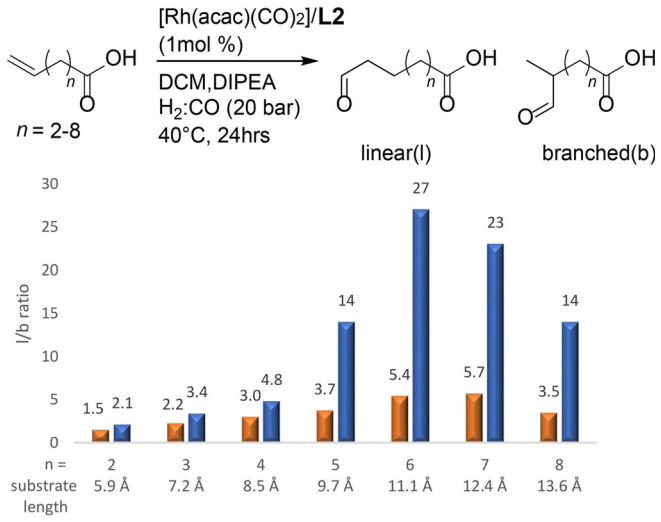

Figure 2. Hydroformylation of ω-unsaturated carboxylic acids using rhodium complexes based on **L2**.[a] [a] Reagents and conditions: [substrate] = 0.2 M, DIPEA (15 equiv), $[Rh(acac)(CO)_2]$ (1 mol%), **L2** (1.1 mol%), 20 bar CO/H_2 (1:1), 40 °C, 24 h. Conversion and regioselectivity determined by ^1H NMR analysis of the crude reaction mixture. For full experimental details, see the Supporting Information. The blue bars are experiments in presence of base, and the orange bars are in absence of base as control experiment.

Table 1. Selective hydroformylation of 8-decenoic acid and 9-undecenoic acid.[a]

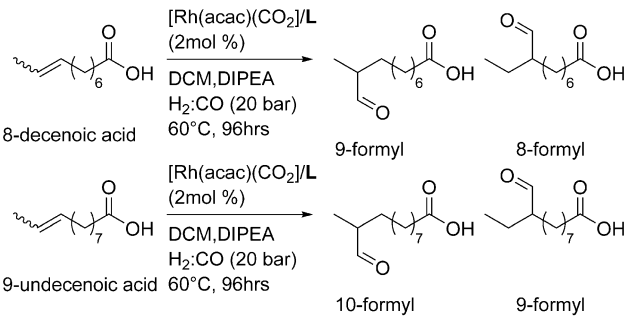

Substrate	Ligand	Conversion [%]	9-Formyl/ 8-formyl	9-Formyl/ all other isomers
8-decenoic acid	**L1**	74	2.6	1.9
8-decenoic acid	**L2**	97	8.8	5.8
8-decenoic acid	PPh_3	100	1.6	1.6

Substrate	Ligand	Conversion [%]	10-Formyl/ 9-formyl	10-Formyl/ all other isomers
9-undecenoic acid	**L1**	70	2.2	1.7
9-undecenoic acid	**L2**	96	6.9	5.0
9-undecenoic acid	PPh_3	100	1.3	1.3

[a] Reagents and conditions: [substrate] = 0.2 M, DIPEA (1.5 equiv), $[Rh(acac)(CO)_2]$ (2 mol%), **L1** and **L2** (2.2 mol%), PPh_3 (6.6 mol%), 20 bar CO/H_2 (1:1), 60 °C, 96 h. Conversion and regioselectivity determined by ^1H NMR analysis of the reaction mixture. For full experimental details, see the Supporting Information.

tance. The highest l/b ratio of 27 is obtained for the 8-nonenoate ($n = 6$), which is the substrate that binds strongest to the catalyst as it fits perfectly according to our modelling studies (vide supra). The longer substrates that easily span the distance between the DIM pocket and the rhodium center ($n = 7$ and 8) are also converted with improved regioselectivity when preorganized, albeit with a lower linear/branched ratio of 23 and 14, respectively, in line with the binding energy calculated for these substrates. The smaller substrates ($n = 2$ and 3) are not able to bind in a ditopic fashion to [Rh(**L2**)] and thus the difference in l/b ratios between the anionic and the protonated substrates is very small. Consistent with our design model, the **L2** system is indeed more selective than the **L1** system for long substrates (e.g. 9-decenoate: l/b of 7/1 for **L1** and l/b 23/1 for **L2**, see Figure S18 for full comparison of l/b ratios of **L1** and **L2**).[21]

We continued our catalytic studies using internal alkenes with a remote carboxylate group as substrates, which served as models for natural monounsaturated fatty acids that possess an internal double bond at the Δ9-position. Initial investigations were conducted with 8-decenoate, which is the internal alkene analogue of the most selective terminal alkene substrate (vide supra), and 9-undecenoate, which has the exact alkene-carboxylic acid distance as natural fatty acids (Table 1).[9,10,21]

When 8-decenoate was hydroformylated using the PPh_3-based catalyst the two aldehyde products were formed with a small excess for the 9-formyl product.[9,10,21,39] Performing the same reaction with the rhodium catalyst based on **L2** that preorganizes the substrate leads to high conversion with a high regioselectivity to produce the 9-formyl product in excess (9-formyl/8-formyl ratio is 8.8).

The linear aldehyde product is also observed under these conditions, which arises from an isomerization/hydroformylation sequence, which is not uncommon for bisphosphite-based catalysts.[47] When we applied the rhodium catalyst based on **L1**, the catalyst that can also pre-organize but is optimized for smaller substrates, only slightly better selectivities are obtained than with the PPh_3-based catalysts. The same trend was observed in the hydroformylation of 9-undecenoic acid; only the [Rh(**L2**)] catalyst provides the product with high regioselectivity, yielding a 10-formyl/9-formyl ratio of 6.9. Importantly, the redesigned [Rh(**L2**)] catalyst clearly outcompetes [Rh(**L1**)] with respect to regioselectivity and conversion for the longer substrates, as a result of more favorable ditopic binding.

Having established our redesigned [Rh(**L2**)] catalyst is able to control the regioselectivity of remote internal alkenes on position Δ8 and Δ9 through preorganization, we extended our system to naturally occurring monounsaturated fatty acids (oleic acid, palmitoleic acid and myristoleic acid, Table 2). When myristoleic acid is hydroformylated using the PPh_3-based rhodium catalyst, equal amounts of the 10-formyl and the 9-formyl products are formed, in line with previous reports.[39–41] Furthermore, when the same reaction was carried out with the [Rh(**L1**)] catalyst, also equal amounts of the two regioisomers are obtained. In contrast, the [Rh(**L2**)] catalyst provides a 10-formyl/9-formyl ratio of 1.61 and shows this catalyst can con-

Table 2. Hydroformylation of natural fatty acids.[a]

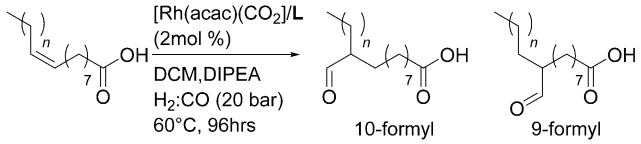

n=3, myristoleic acid
n=5, palmitoleic acid
n=7, oleic acid

	Ligand	Conversion [%]	10-Formyl/ 9-formyl	10-Formyl/ all other isomers
myristoleic acid	**L1**	27	1.03	0.79
myristoleic acid	**L2**	69	1.61	1.23
myristoleic acid	PPh_3	100	1.0	1.0
palmitoleic acid[b]	**L1**	23	≈1.0	≈0.8
palmitoleic acid[b]	**L2**	66	≈1.5	≈1.2
palmitoleic acid[b]	PPh_3	100	≈1.0	≈1.0
oleic acid[c]	**L1**	21	n.d.	n.d.
oleic acid[c]	**L2**	76	n.d.	n.d.
oleic acid[c]	PPh_3	100	n.d.	n.d.

[a] Reagents and conditions: [substrate] = 0.2 M, DIPEA (1.5 equiv), [Rh(acac)$(CO)_2$] (2 mol%), **L1** and **L2** (2.2 mol%), PPh_3 (6.6 mol%), 20 bar CO/H_2 (1:1), 60 °C, 96 h. Conversion determined by ^{1}H NMR analysis of the reaction mixture and the regioselectivity was determined by GC analysis after methylation of the reaction mixture. [b] Methyl 9- and 10-formylpalmitate could not be baseline separated on GC, therefore a larger error in the determined regioselectivity is expected. [c] 9- and 10-formyl stearic acid were not separable after methylation on GC and therefore the regioselectivity was not determined (n.d.). For full experimental details, see the Supporting Information.

Table 3. Optimization of regioselectivity of myristoleic acid.[a]

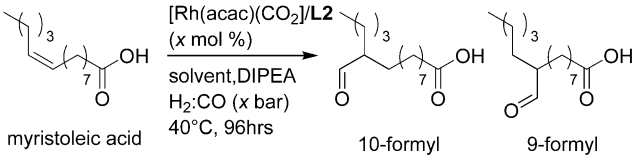

Entry	[Substrate] [M]	[Catalyst] [mM]	Conversion [%]	10-/9-Formyl tetradecanoic acid	10-Formyl tetradecanoic acid/all other isomers
1	0.2	4	33	1.87	1.58
2	0.1	4	66	1.99	1.61
3	0.02	4	85	2.20	1.72
4	0.02	0.4	76	2.31	1.90
5[b]	0.2	4	35	1.82	1.63
6[b]	0.02	0.4	77	2.43	1.95
7[c]	0.02	0.4	20	1.42	1.42
8[d]	0.02	0.4	>1	n.d.	n.d.
9[e]	0.2	4	32	2.10	1.91
10[e]	0.02	0.4	63	2.51	2.33

[a] Reagents and conditions: DCM, DIPEA (1.5 equiv with respect to acid), catalyst = [Rh(acac)$(CO)_2$]/**L2** in a 1:1.1 ratio, substrate = myristoleic acid, 20 bar CO/H_2 (1:1), 40 °C, 96 h. Conversion determined by ^{1}H NMR analysis of the reaction mixture and the regioselectivity was determined via GC analysis following methylation of the reaction mixture. [b] Rhodium:ligand ratio 1:2. [c] THF used as solvent instead of DCM [d] DMF was used instead of DCM. For full experimental details, see the Supporting Information. [e] 50 bar syngas (H_2:CO)(1:1) was used instead of 20 bar of syngas.

trol the regioselectivity of this substrate via substrate preorganization. For the fatty acids also minor amounts of isomerization/hydroformylation products were observed with the [Rh(**L1**)] and [Rh(**L2**)] catalysts, lowering the overall selectivity.

Palmitoleic acid was converted with similar levels of regioselectivity as observed for myristoleic acid, with the [Rh(**L2**)] catalyst being the only catalyst capable of controlling the regioselectivity (10-formyl/9-formyl ratio is ≈1.5 for [Rh(**L2**)] and ≈1.0 for [Rh(**L1**)] and [Rh(PPh_3)], Table 2). For the fatty acids also minor amounts of isomerization/hydroformylation products were observed with the [Rh(**L1**)] and [Rh(**L2**)] catalysts, lowering the overall selectivity. Palmitoleic acid was converted with similar levels of regioselectivity as observed for myristoleic acid, with the [Rh(**L2**)] catalyst being the only catalyst capable of controlling the regioselectivity (10-formyl/9-formyl ratio is ≈1.5 for [Rh(**L2**)] and ≈1.0 for [Rh(**L1**)] and [Rh(PPh_3)](Table 2)). A major platform chemical, oleic acid, was also hydroformylated using these catalysts. Similar conversion was observed with oleic acid as with myristoleic acid and palmitoleic acid using the respective catalysts. However, the regioisomers could not be separated on GC and therefore the regioselectivity could not be determined.

With a regioselective hydroformylation catalyst for monounsaturated fatty acids in hand, we optimized the reaction conditions using myristoleic acid as a substrate to further improve the selectivity (Table 3). We commenced our optimization studies by lowering the reaction temperature to 40 °C. This resulted in an improvement of 10-formyl/9-formyl ratio from 1.61 to 1.87, although at a lower conversion (69% vs. 33%) (see entry 1 of Table 3). Under the same conditions (40 °C) but at lower substrate concentrations (compare entries 1–3) the regioselectivity was further enhanced yielding 10-formyl/9-formyl ratios of 1.99 and 2.20 at a substrate concentration of 0.1 M and 0.02 M, respectively. Most likely, the lower selectivity at higher substrate concentration results from unselective hydroformylation reactions in which the substrate is not ditopically bound, which is more dominant at higher substrate concentrations, especially for these longer substrates.[21,48,49] In the experiment where the catalyst concentration was reduced by a factor 10 (entry 4) the regioselectivity further increased (10-formyl/9-formyl ratio to 2.31). Somewhat counterintuitively, the conversion was also higher in the experiment, reflecting the complicated kinetics of the system. Such complicated kinetics was previously reported for [Rh(**L1**)], in which the catalytically active species is in equilibrium with dormant state complexes in which carboxylate groups of the substrate and product are directly coordinated to rhodium.[23,50] Increasing the rhodium:ligand ratio from 1:1.1 to 1:2 (entries 5 and 6) further improved the regioselectivity to yield a 10-formyl/9-formyl ratio of 2.43 under dilute conditions (entry 6). Changing the solvent from DCM to THF or DMF (entries 7 and 8) led to lower activity and selectivity. Experiments performed at syngas pressures of 50 bar instead of 20 bar (entries 9 and 10), but otherwise identical conditions, led to an improved regioselectivity of 2.10 and 2.51 for entries 9 and 10 respectively. Notably, also the overall selectivity improved to 1.91 and 2.33 respectively, which is ex-

plained by lower levels of isomerization of the alkene, commonly observed for hydroformylation reactions carried out at higher CO concentration.[51]

In conclusion, supramolecular substrate orientation is a powerful tool to control selectivity in transition metal catalysis, which has been mainly demonstrated for substrates in which the supramolecular functional group is close to the reactive group. In this paper, we demonstrate that supramolecular substrate orientation can also work when this group is remote from the reactive group, thereby increasing the scope of the approach. In order to show this a previously reported hydroformylation catalyst with an integrated anion receptor, DIMPhos [Rh(**L1**)], was redesigned to accommodate larger substrates. This hydroformylation catalyst ([Rh(**L2**)]) converts substrates with high regioselectivity when the carboxylate directing group is remote from the alkene group, including monounsaturated fatty acids (MUFAs) and their model substrates. The [Rh(**L2**)] catalyst provides the hydroformylation product with a 10-formyl/9-formyl ratio of 2.51 for myristoleic acid, which represents the first selective catalyst for this biobased compound. These results show that catalysts that operate via supramolecular substrate preorganization can be redesigned to provide selective catalysts for substrates of different sizes, and as such we are able to make a catalyst that can convert fatty acids in a regioselective fashion. This paves the way for the design of other challenging conversions for which no catalysts exist yet.

Acknowledgements

NWO, the Dutch science foundation, is acknowledged for financial support. We also would like to thank InCatT for financial support and useful discussions.

Conflict of interest

The authors declare no conflict of interest.

Keywords: fatty acid functionalization · hydroformylation · regioselectivity · substrate preorganization · supramolecular chemistry

[1] H. J. Davis, R. J. Phipps, *Chem. Sci.* **2017**, *8*, 864 – 877.
[2] J. Meeuwissen, J. N. H. Reek, *Nat. Chem.* **2010**, *2*, 615 – 621.
[3] P. Dydio, J. N. H. Reek, *Chem. Sci.* **2014**, *5*, 2135 – 2145.
[4] S. S. Nurttila, P. R. Linnebank, T. Krachko, J. N. H. Reek, *ACS Catal.* **2018**, *8*, 3469 – 3488.
[5] M. Raynal, P. Ballester, A. Vidal-Ferran, P. W. N. M. van Leeuwen, *Chem. Soc. Rev.* **2014**, *43*, 1660 – 1733.
[6] M. Raynal, P. Ballester, A. Vidal-Ferran, P. W. N. M. van Leeuwen, *Chem. Soc. Rev.* **2014**, *43*, 1734 – 1787.
[7] D. M. Vriezema, M. C. Aragonès, J. A. A. W. Elemans, J. J. L. M. Cornelissen, A. E. Rowan, R. J. M. Nolte, *Chem. Rev.* **2005**, *105*, 1445 – 1489.
[8] D. Vidal, G. Olivo, M. Costas, *Chem. Eur. J.* **2018**, *24*, 5042 – 5054.
[9] V. F. Slagt, J. N. H. Reek, P. C. J. Kamer, P. W. N. M. Van Leeuwen, *Angew. Chem. Int. Ed.* **2001**, *40*, 4271 – 4274; *Angew. Chem.* **2001**, *113*, 4401 – 4404.
[10] M. Kuil, T. Soltner, P. W. N. M. Van Leeuwen, J. N. H. Reek, *J. Am. Chem. Soc.* **2006**, *128*, 11344 – 11345.
[11] T. Gadzikwa, R. Bellini, H. L. Dekker, J. N. H. Reek, *J. Am. Chem. Soc.* **2012**, *134*, 2860 – 2863.
[12] M. Yoshizawa, M. Tamura, M. Fujita, *Science* **2006**, *312*, 251 – 254.
[13] Y. Kuninobu, H. Ida, M. Nishi, M. Kanai, *Nat. Chem.* **2015**, *7*, 712 – 717.
[14] H. J. Davis, M. T. Mihai, R. J. Phipps, *J. Am. Chem. Soc.* **2016**, *138*, 12759 – 12762.
[15] R. Breslow, X. Zhang, R. Xu, M. Maletic, R. Merger, *J. Am. Chem. Soc.* **1996**, *118*, 11678 – 11679.
[16] T. A. Bender, R. G. Bergman, K. N. Raymond, F. D. Toste, *J. Am. Chem. Soc.* **2019**, *141*, 11806 – 11810.
[17] A. Bauer, F. Westkämper, S. Grimme, T. Bach, *Nature* **2005**, *436*, 1139 – 1140.
[18] P. A. Lichtor, S. J. Miller, *Nat. Chem.* **2012**, *4*, 990 – 995.
[19] S. Das, C. D. Incarvito, R. H. Crabtree, G. W. Brudvig, *Science* **2006**, *312*, 1941 – 1943.
[20] P. Dydio, W. I. Dzik, M. Lutz, B. de Bruin, J. N. H. Reek, *Angew. Chem. Int. Ed.* **2011**, *50*, 396 – 400; *Angew. Chem.* **2011**, *123*, 416 – 420.
[21] P. Dydio, J. N. H. Reek, *Angew. Chem. Int. Ed.* **2013**, *52*, 3878 – 3882; *Angew. Chem.* **2013**, *125*, 3970 – 3974.
[22] P. Dydio, R. J. Detz, J. N. H. Reek, *J. Am. Chem. Soc.* **2013**, *135*, 10817 – 10828.
[23] P. Dydio, R. J. Detz, B. de Bruin, J. N. H. Reek, *J. Am. Chem. Soc.* **2014**, *136*, 8418 – 8429.
[24] T. Šmejkal, B. Breit, *Angew. Chem. Int. Ed.* **2008**, *47*, 311 – 315; *Angew. Chem.* **2008**, *120*, 317 – 321.
[25] W. Fang, B. Breit, *Angew. Chem. Int. Ed.* **2018**, *57*, 14817 – 14821; *Angew. Chem.* **2018**, *130*, 15033 – 15037.
[26] S. T. Bai, V. Sinha, A. M. Kluwer, P. R. Linnebank, Z. Abiri, B. de Bruin, J. N. H. Reek, *ChemCatChem* **2019**, *11*, 5322 – 5329.
[27] S. Perdriau, S. Harder, H. J. Heeres, J. G. de Vries, *ChemSusChem* **2012**, *5*, 2427 – 2434.
[28] G. Olivo, G. Farinelli, A. Barbieri, O. Lanzalunga, S. Di Stefano, M. Costas, *Angew. Chem. Int. Ed.* **2017**, *56*, 16347 – 16351; *Angew. Chem.* **2017**, *129*, 16565 – 16569.
[29] P. Dydio, T. Zieliński, J. Jurczak, *Chem. Commun.* **2009**, 4560 – 4562.
[30] D. R. Dodds, R. A. Gross, *Science* **2007**, *318*, 1250 – 1251.
[31] P. J. Deuss, K. Barta, J. G. De Vries, *Catal. Sci. Technol.* **2014**, *4*, 1174 – 1196.
[32] T. Vanbésien, E. Monflier, F. Hapiot, *Eur. J. Lipid Sci. Technol.* **2016**, *118*, 26 – 35.
[33] A. Behr, D. Obst, A. Westfechtel, *Eur. J. Lipid Sci. Technol.* **2005**, *107*, 213 – 219.
[34] P. N. R. Vennestrøm, C. M. Osmundsen, C. H. Christensen, E. Taarning, *Angew. Chem. Int. Ed.* **2011**, *50*, 10502 – 10509; *Angew. Chem.* **2011**, *123*, 10686 – 10694.
[35] S. Pandey, D. R. Shinde, S. H. Chikkali, *ChemCatChem* **2017**, *9*, 3997 – 4004.
[36] T. Seidensticker, A. J. Vorholt, A. Behr, *Eur. J. Lipid Sci. Technol.* **2016**, *118*, 3 – 25.
[37] S. Pandey, S. H. Chikkali, *ChemCatChem* **2015**, *7*, 3468 – 3471.
[38] K. F. Muilwijk, P. C. J. Kamer, P. W. N. M. van Leeuwen, *J. Am. Oil Chem. Soc.* **1997**, *74*, 223 – 228.
[39] E. N. Frankel, *J. Am. Oil Chem. Soc.* **1971**, *48*, 248 – 253.
[40] E. Benetskiy, S. Lühr, M. Vilches-Herrera, D. Selent, H. Jiao, L. Domke, K. Dyballa, R. Franke, A. Börner, *ACS Catal.* **2014**, *4*, 2130 – 2136.
[41] J. Boulanger, A. Ponchel, H. Bricout, F. Hapiot, E. Monflier, *Eur. J. Lipid Sci. Technol.* **2012**, *114*, 1439 – 1446.
[42] T. Gaide, J. Bianga, K. Schlipköter, A. J. Vorholt, *ACS Catal.* **2017**, *7*, 4163 – 4171.
[43] G. te Velde, F. M. Bickelhaupt, E. J. Baerends, C. Fonseca Guerra, S. J. A. van Gisbergen, J. G. Snijders, T. Ziegler, *J. Comput. Chem.* **2001**, *22*, 931 – 967.
[44] Amsterdam Modeling Suite, Software for Chemistry and Materials, http://www.scm.com.
[45] E. van Lenthe, A. Ehlers, E.-J. Baerends, *J. Chem. Phys.* **1999**, *110*, 8943 – 8953.
[46] R. Gramage-Doria, J. Hessels, S. H. A. M. Leenders, O. Tröppner, M. Dürr, I. Ivanović-Burmazović, J. N. H. Reek, *Angew. Chem. Int. Ed.* **2014**, *53*, 13380 – 13384; *Angew. Chem.* **2014**, *126*, 13598 – 13602.
[47] A. Van Rooy, P. C. J. Kamer, P. W. N. M. Van Leeuwen, K. Goubitz, J. Fraanje, N. Veldman, A. L. Spek, *Organometallics* **1996**, *15*, 835 – 847.

[48] A. Mulder, J. Huskens, D. N. Reinhoudt, *Org. Biomol. Chem.* **2004**, *2*, 3409 – 3424.
[49] The effective concentration for substrate *x* bound in the DIM pocket was roughly estimated: The maximum radius between the rhodium center and the double bond of natural fatty acids is approximately 11 Å which is 1.1×10^{-8}dm^3. Which translates to $4/3\pi(1.1\times10^{-8}\text{dm})^3=5.5\times10^{-24}$ dm^3. Of this spherical volume it was estimated the alkene could occupy 50%. This translates to an effective concentration of $\approx$0.6 M. Since the substrate concentration is 0.2 M for most experiments, non-bound substrates will likely compete and allow for a non-selective background reaction. This nicely explains why the regioselectivity increases upon lowering of the concentration as this background reaction is repressed.
[50] E. Mieczyńska, A. M. Trzeciak, J. J. Ziółkowski, *J. Mol. Catal.* **1993**, *80*, 189 – 200.
[51] R. Franke, D. Selent, A. Börner, *Chem. Rev.* **2012**, *112*, 5675 – 5732.

Manuscript received: February 5, 2020
Accepted manuscript online: March 21, 2020
Version of record online: June 11, 2020